Pergamon

Journal of Structural Geology, Vol. 16, No. 8, pp. 1159 to 1172, 1994

0191-8141/94 $07.00+0.00

0191-8141(93) E0018-G

Flow variation in layered rocks subjected to bulk flow of various kinematic vorticities: theory and geological implications

DAZHI JIANG

Department of Geology, University of New Brunswick, PO Box 4400, Fredericton, N.B., Canada E3B 5A3

(*Received* 27 *April* 1993; *accepted in revised form* 4 *November* 1993)

Abstract—Flow variation is studied analytically in rocks with layers of varied competence and varied orientation with respect to constant bulk flow fields of given kinematic vorticity ($0 \leq W_k \leq 1$). The results explicitly demonstrate that flow varies significantly from layer to layer and with time in any individual layer even though the bulk flow is constant. Any flow regime can occur and the instantaneous stretching axes (ISA) spin all the time. Reverse sense of non-coaxiality can occur in the same layer at different times and in different layers at the same time. This study further reveals the significance of heterogeneity and non-steadiness in natural flows. The assumption of a time-independent flow history for natural deformation is highly unrealistic. The spinning of the instantaneous stretching axes (ISA) and the variation of flow regimes have bearings on the progressive development of fabrics and structures such as folded boudins, refolded folds in shear zones and double rotation of porphyroclasts that are often interpreted as being due to multi-deformational events.

INTRODUCTION

IN CONTRAST to the abundant studies of natural finite strain, studies on the deformation path by which the final deformation is achieved are rare. For example, the variation of deformation across competence contrast boundaries has received the attention of geologists for over a century, and many theoretical and experimental studies have been done in the field of finite strain (e.g. Treagus 1983, 1988, 1993 and references therein, Ramsay 1982, Ramsay & Huber 1983) and more recently on the refraction of stress and strain rate across competence boundaries (Treagus 1993). But, as far as I am aware, Ishii's (1992) work is the only theoretical investigation of deformation path in this connection. Time-independent flow histories are often assumed implicitly or explicitly to fill the gap between the initial (undeformed) state and the final (deformed) state. When the structure or fabric geometry presents some degree of obliquity, a non-coaxial (simple shear or sub-simple shear flow) history is assumed, otherwise a coaxial (pure shear) flow history is assumed. However, the real deformation path of rocks may be far more complex (see e.g. Lister & Williams 1979, 1983, Williams & Schoneveld 1981, Celma 1982, Choukroune *et al.* 1987). The development of geological structures and fabrics is intimately related to the deformation path. In order to increase our understanding of the processes involved in natural deformations, possible flow histories and associated deformation paths need to be determined.

In this paper, I investigate analytically how flow varies in layered rocks as they undergo constant bulk flows of different kinematic vorticity number ($0 \leqslant W_k \leqslant 1$). It will be shown that even if the bulk flows are constant, flow varies both from layer to layer (heterogeneity) and in the same layer with time (non-steadiness). Any flow regime, including super-simple shear, can occur. Unlike previous studies, the rheology of rock is not assumed and perfect adherence between layers is not required.

Since flow terminology and concepts are referred to throughout the paper, a synoptic summary of flow theory is first given. This is followed by a consideration of the description of competence contrast between layers. The theoretical results of flow variation in layers of different competence is then presented and the mathematical derivation of the instantaneous velocity gradient tensors is given in the Appendix. The paper concludes with a discussion on the geological implications of this study.

SYNOPTIC SUMMARY OF FLOW FIELD THEORY

Flow classification

Flow is described by the velocity (**v**) of all particles in a medium. The velocity can be expressed (Ottino 1989, pp. 28–30) in terms of either particle (**X**)—Lagrangian or material velocity—or spatial location (**x**)—Eulerian or spatial velocity, i.e.:

$$\mathbf{v} = \mathbf{v}(\mathbf{X},t) \quad \text{Lagrangian or material}$$
$$\mathbf{v} = \mathbf{v}(\mathbf{x},t) \quad \text{Eulerian or spatial.} \qquad (1)$$

From the velocity, three quantities are derived, namely *gradient*, *divergence* and *curl*.

The Eulerian *gradient* of **v** is often called the instantaneous velocity gradient tensor (**L** = grad **v**) whose components are:

$$L_{ij} = \frac{\partial v_i}{\partial x_j} (i,j = 1,2,3). \qquad (2)$$

The *divergence* of **v** is commonly called the rate of

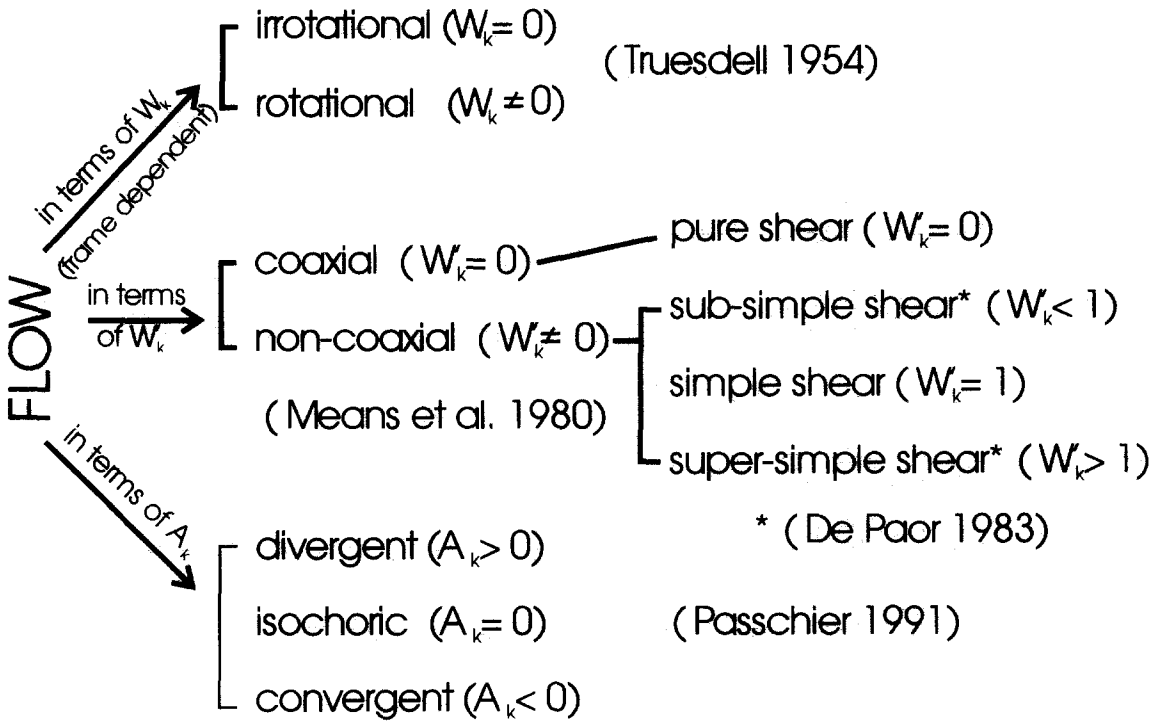

Fig. 1. Flow classification based on different parameters. See text for details.

dilation or rate of volume change (Δ) (see Sedov 1971, p. 124):

$$\Delta = \operatorname{div} \mathbf{v} = \frac{1}{\Delta V}\frac{\mathrm{d}\Delta V}{\mathrm{d}t} = \frac{\partial v_1}{\partial x_1} + \frac{\partial v_2}{\partial x_2} + \frac{\partial v_3}{\partial x_3} = \operatorname{tr}[\mathbf{L}], \quad (3)$$

where ΔV is an infinitesimal volume at a point. For isochoric flow $\Delta \equiv 0$.

The *curl* of $\mathbf{v}$ is the instantaneous vorticity vector:

$$\mathbf{w} = \operatorname{curl} \mathbf{v} = \left(\mathbf{i}\frac{\partial}{\partial x_1} + \mathbf{j}\frac{\partial}{\partial x_2} + \mathbf{k}\frac{\partial}{\partial x_3}\right) \times \mathbf{v}. \quad (4)$$

On the basis of these three quantities, many parameters have been defined as criteria to classify flow (e.g. Astarita 1976, Tanner 1976), among which are the following.

Truesdell's kinematic vorticity number (W_k)*—measure of instantaneous rotation*. It was defined as (Truesdell 1954):

$$W_k = W \cdot \{2(s_1^2 + s_2^2 + s_3^2)\}^{-1/2}, \quad (5)$$

where W is the magnitude of vorticity vector and s_1, s_2, s_3 ($s_1 \geq s_2 \geq s_3$) are three eigenvalues of the stretching tensor $\mathbf{D}$, whose components are $D_{ij} = \frac{1}{2}(L_{ij} + L_{ji})$ (Truesdell 1954). If $W_k = 0$, the flow is irrotational, otherwise it is rotational.

Means' kinematic vorticity number (W'_k)*—measure of instantaneous non-coaxiality*. Since the vorticity differs in different frames, W_k is frame-dependent. However the vorticity measured in a selected external frame can be partitioned into internal or shear-induced vorticity (W_I) and external vorticity (W_E), or spin (Means *et al.* 1980, Lister & Williams 1983). A frame-independent internal kinematic vorticity number W'_k was defined by Means *et al.* (1980) as a measure of the instantaneous non-coaxiality:

$$W'_k = W_I \cdot \{2(s_1^2 + s_2^2 + s_3^2)\}^{-1/2}. \quad (6)$$

Passchier's kinematic dilatancy number (A_k)*—measure of instantaneous dilatancy*. It was defined as (Passchier 1991a):

$$A_k = \Delta \cdot \{2(s_1^2 + s_2^2 + s_3^2)\}^{-1/2}. \quad (7)$$

Figure 1 shows flow classification based on these parameters. A flow can be well characterized by its attributive parameters. For example, a flow with $W_k = 0$, $W'_k < 1$ and $A_k > 0$ may be called 'irrotational divergent sub-simple shear'.

Eigenvectors and particle paths of steady-state isochoric flow

Particle paths of flow regimes for steady-state isochoric flows have been studied by Ramberg (1975) and Goguel (1979). The Mohr circle construction has been used as a powerful means to describe flow by Lister & Williams (1983), Bobyarchick (1986), Passchier (1988a,b, 1991a) and has recently been reviewed by Simpson & De Paor (1993). Figure 2 summarizes all flow regimes. For super-simple shear ($W_k > 1$) (De Paor 1983), the particle paths form loops. In such a flow, all material lines rotate in the same sense. For $0 \leq W_k \leq 1$, the particle paths are open-ended with two flow eigenvectors (A_1, A_2) (Goguel 1979, Bobyarchick 1986, Passchier 1986, 1987a,b, 1988a, 1990). Material lines parallel to the eigenvectors do not rotate. Material lines lying

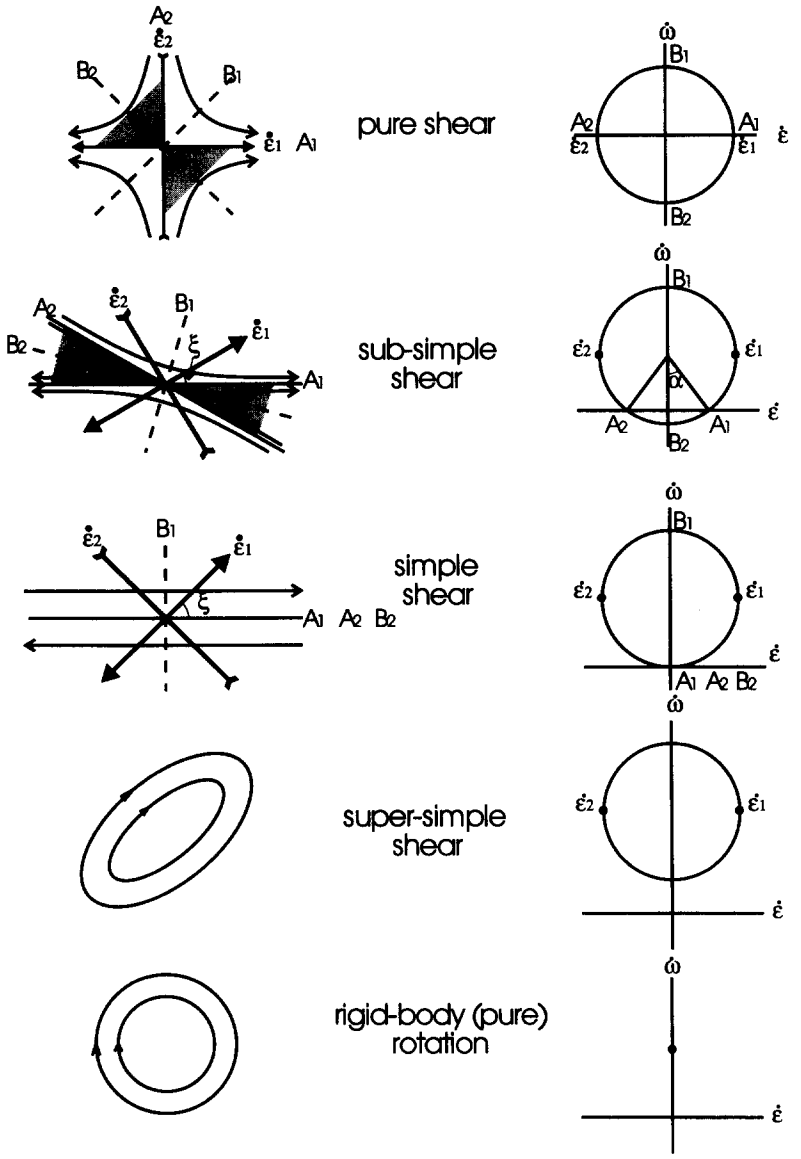

Fig. 2. Steady-state isochoric flow fields and their representation by Mohr circles. A_1, A_2: flow eigenvectors; $\dot{\varepsilon}_1$, $\dot{\varepsilon}_2$: extensional and contractional instantaneous stretching axes (ISA); B_1, B_2: bisectors of forward rotation (blank) and backward rotation (dotted) sectors; α: angle between A_1 and A_2; ξ: angle between $\dot{\varepsilon}_1$ and A_1. W_k is related to α and ξ by the relationship $W_k = \cos\alpha = \sin(2\xi)$. See text for details.

within the obtuse and acute sectors will rotate in opposite senses toward the extensional eigenvector (A_1). Hereafter those rotating in the same sense as the bulk non-coaxiality are referred to as forward rotation (FR) and those rotating in the opposite sense backward rotation (BR). The maximum angular velocities are reached at two bisectors of the obtuse and acute sectors (B_1, B_2) (Ghosh & Ramberg 1976, Bobyarchick 1986, Passchier 1987a,b). These rotational behaviors of material lines have been used in the interpretation of kinematic indicators (Hanmer & Passchier 1991, Simpson & De Paor 1993). The cosine of the angle α between A_1 and A_2 equals the kinematic vorticity of the flow (Bobyarchick 1986). For pure shear flow, A_1 and A_2 are perpendicular; for simple shear, they coincide and for a sub-simple shear $0° < \alpha < 90°$. The instantaneous stretching axes (ISA) are at 45° with respect to B_1 and B_2. The extensional ISA makes an angle ξ with respect to A_1 and sin (2ξ) equals the kinematic vorticity number (Weijermars 1991). These relations can be used to construct a flow field when flow parameters are known.

COMPETENCE CONTRAST BETWEEN LAYERS

When rocks undergo deformation, the interaction between different domains due to their anisotropic and rheological differences induces domainal and time-dependent flow (Jiang 1994). The term *competence contrast* has been used qualitatively to describe the variation of deformation features as a result of such differential flow histories (e.g. Ramsay 1982, Ramsay & Huber 1983, p. 12, Twiss & Moores 1992, p. 239). It is evident that a more quantitative treatment of competence contrast lies in the different constitutive equations that have governed the flow in different rock

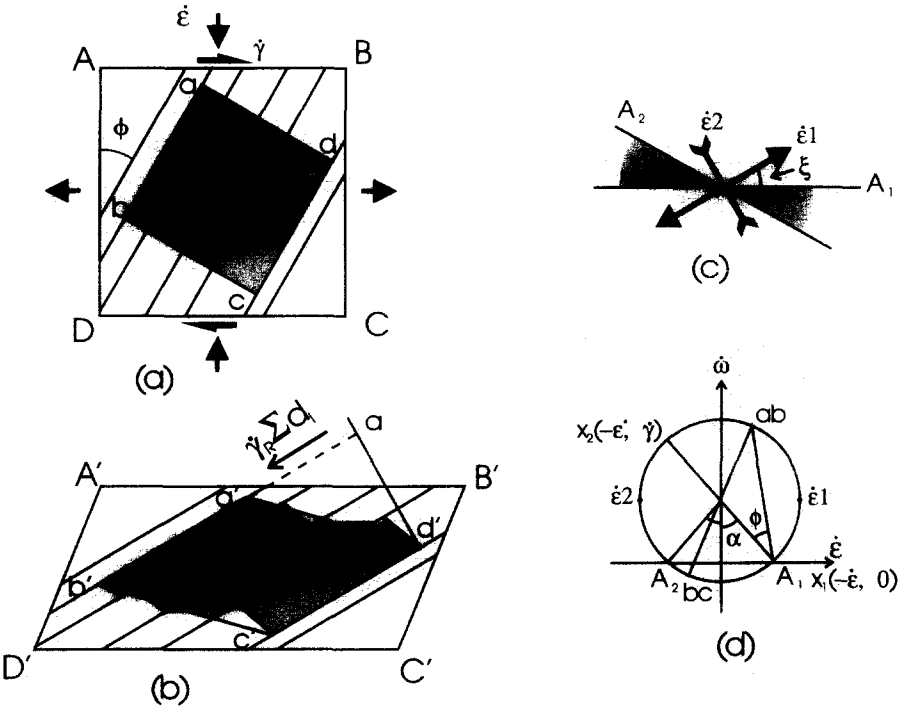

Fig. 3. Layers of varied competence at an arbitrary orientation with respect to a steady-state isochoric bulk flow with a pure shear component and simple shear component of $\dot{\epsilon}$ and $\dot{\gamma}$, respectively. (a) The ϕ-configuration; abcd is a square; the orientation of the extensional ISA of the flow in a given layer is designated by θ. (b) After an incremental deformation of (a), ad becomes a'd', which is a 'broken zigzag' due to the competence difference between layers and slip along layer boundaries. The displacement rate of ab to cd is $\dot{\gamma}_R \Sigma d_i$. (c) Bulk flow field. (d) Mohr circle of the bulk flow. The resolved shear strain rate parallel to the layer ab is $\dot{\gamma}_R = \dot{\omega}_{ab} - \dot{\omega}_{bc}$. See text for details.

domains. Some authors have tried to relate the concept of competence to parameters describing mechanical properties of rocks such as strength (e.g. Hobbs *et al.* 1976, Means 1990) or viscosity (Cobbold 1983, Treagus 1983, 1988, Ishii 1992). This is viable only when different domains are of the same rheology (elastic, linear viscous, power-law with the same stress exponent, etc.) so that constitutive equation differences can be simplified to differences in common mechanical parameters like Young's modulus, viscosity and power-law coefficients. To illustrate this, Tullis *et al.* (1991) have shown that difference in the stress exponent between the flow laws of plagioclase and pyroxene results in their complex relative competence. At high strain rate and low temperature pyroxene is more competent, whereas at low strain rate and high temperature plagioclase is more competent.

For layered rocks, it is observed that different layers often exhibit approximately the same layer-parallel shortening or extension, suggesting approximately the same layer-parallel stretching rates during deformation. What differ between layers are usually their layer-parallel shear strains, indicating different layer-parallel shear strain rates (see Price & Cosgrove 1990, pp. 453–454, Treagus & Sokoutis 1992). To the first approximation, this can be used as a constraint to make the competence contrast between layers relatively easy to deal with. From a phenomenological point of view, each layer is given a *competence factor N* to quantify its competence in this paper. This is defined as (Fig. 3):

$$N = \frac{\text{layer-parallel shear strain rate of the } i\text{th layer}}{\text{resolved shear strain rate parallel to the layer}} = \frac{\dot{\gamma}_i}{\dot{\gamma}_R}. \quad (8)$$

If $0 \leq N < 1$, the layer is accommodating less shear strain rate than what is resolved and it is relatively competent. The smaller N, the more competent the layer. If $1 \leq N < +\infty$, the layer is accommodating the same or more shear strain rate than what is resolved and it is relatively incompetent. The larger N, the more incompetent the layer. As illustrated in Fig. 3, the resolved shear strain rate parallel to the layer (ab) is $\dot{\gamma}_R$, which is easily obtained from the Mohr circle construction (Fig. 3d). The layer-parallel shear strain rates of different layers are $\dot{\gamma}_i (i = 1, 2, 3, \ldots)$. Using d_i to denote the instantaneous thickness of layers, the relative displacement rate between ab and cd due to bulk flow is $\dot{\gamma}_R \Sigma d_i$. This is accommodated by two components. One is the internal shear straining of the layers, which contributes a displacement rate of $\Sigma \dot{\gamma}_i d_i$, and the other is the discontinuous slips on layer boundaries, which contribute a total displacement rate of Σv_i (v_i denotes the slip rates). Therefore we have:

$$\dot{\gamma}_R \sum d_i = \sum v_i + \sum \dot{\gamma}_i d_i.$$

Incorporating (8) and after arrangement, we have:

$$\frac{\sum \left(d_i N_i + \frac{v_i}{\dot{\gamma}_R} \right)}{\sum d_i} = 1$$

or

$$\sum \lambda_i N_i + \frac{\sum \frac{v_i}{\dot{\gamma}_R}}{\sum d_i} = 1, \quad (9)$$

where λ_i is the fractional thickness of the ith layer. Equation (9) specifies the interaction between layers: to achieve a given bulk flow, layer-parallel shear strain rates in different layers and discontinuous slip along competence boundaries must be complementary. When the bulk flow is pure shear and the layers happen to be parallel to one axis of principal strain rate, the resolved shear strain rate and the layer-parallel shear strain rate are both 0, which makes the competence factor indeterminate. This can be explained by the lack of interaction between layers—each layer is deforming the same way as if no other layers exist.

The competence contrast between the ith layer and the jth layer can be described by the ratio of their competence factors:

$$\frac{N_i}{N_j} = \frac{\dot{\gamma}_i}{\dot{\gamma}_j}. \quad (10)$$

Since the shear stress across a competence boundary, irrespective of adherence, must be the same, in the case of Newtonian rheology with viscosity η, we have:

$$\frac{N_i}{N_j} = \frac{\dot{\gamma}_i}{\dot{\gamma}_j} = \frac{\eta_j}{\eta_i}. \quad (11)$$

If the above ratio is time-independent, we have:

$$\frac{\eta_j}{\eta_i} = \frac{\int \dot{\gamma}_i dt}{\int \dot{\gamma}_j dt} = \frac{\gamma_i}{\gamma_j}. \quad (12)$$

This is what has been called the rule of *strain refraction* (Cobbold 1983, Treagus 1983, 1988, Kanagawa 1993).

If the competence contrast as defined in equation (10) is constant during a deformation, despite the rheology of the rock, we have:

$$\frac{N_i}{N_j} = \frac{\gamma_i}{\gamma_j}. \quad (13)$$

This shows that although N may be time-dependent, the layer-parallel finite shear strain ratio can be viewed as the average competence contrast during a deformation.

FLOW VARIATION IN LAYERS OF VARIED N: RESULTS

The derivation of the instantaneous velocity gradient tensor $\mathbf{L}(t)$ is given in the Appendix. From $\mathbf{L}(t)$, all the flow parameters can be calculated (see Jiang 1994). The results are presented here.

The spin of the instantaneous stretching axes (ISA)

The variation of the orientation of ISA in an individual layer (θ, Fig. 3a) vs the instantaneous orientation of the layer (ϕ) is shown in Figs. 4 and 5. The ISA spin within the sector of $\xi - \delta \leq \theta \leq \xi + \delta$. The deviation δ is solely determined by the competence factor of the layer: the more deviant the competence factor from 1, the bigger δ (Fig. 6). θ is equal to ξ in all layers if they are parallel to any of the following 'eigen' directions of the bulk flow: two bulk ISA, B_1 and B_2. Between these directions the variation of θ in competent and incompetent layers presents an inverse relationship—when θ in an incompetent layer is larger than ξ, θ in a competent layer will be smaller than ξ and vice versa (Figs. 4 and 5).

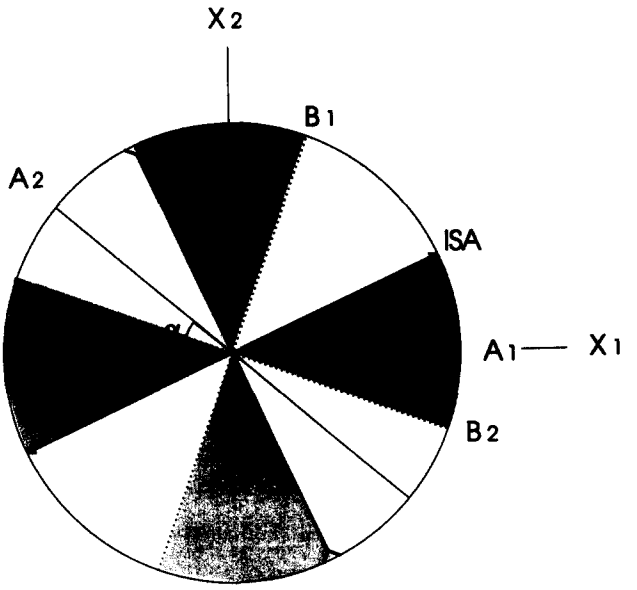

Fig. 4. The orientations (θ) of the ISA in layers are the same as the orientations of the bulk ISA ($\theta = \xi$), irrespective of their N, when layers are parallel to B_1, B_2, and two bulk ISA. If layers are in the dotted sectors, for incompetent layers $\theta > \xi$, while for competent layers, $\theta < \xi$. The situation is vice versa in the blank sectors.

The sense and rate of spin versus ϕ is presented in Fig. 7. It is readily seen that the curves fall into forward rotation (FR) and backward rotation (BR) sectors with B_1 and B_2 as their symmetric lines, respectively. For incompetent layers in the BR sector, both spin and the sense of rotation of the layers are backward with maximum spin rate at B_2. In the FR sector layers rotate forward but the sense of spin is complicated: maximum forward spin is achieved at B_1, but near two eigenvectors, the spin is backward. For competent layers, unless $N = 0$ spin is not necessarily of the same sense as the rotation of the layer. Around both B_1 and B_2 spin is opposite to the sense of rotation of the layer.

Variation of the internal vorticity

The variation of the internal vorticity is presented in Fig. 8. For incompetent layers, in the BR sector the sense of shear is always sympathetic to the bulk sense of shear with maximum shear strain rate at B_2. In the FR sector a reverse sense of shear may or may not occur depending on the bulk kinematic vorticity number and how incompetent the layer is. The higher the bulk kinematic vorticity number, i.e. the stronger the bulk non-coaxiality, the less likely is reverse shear, whereas

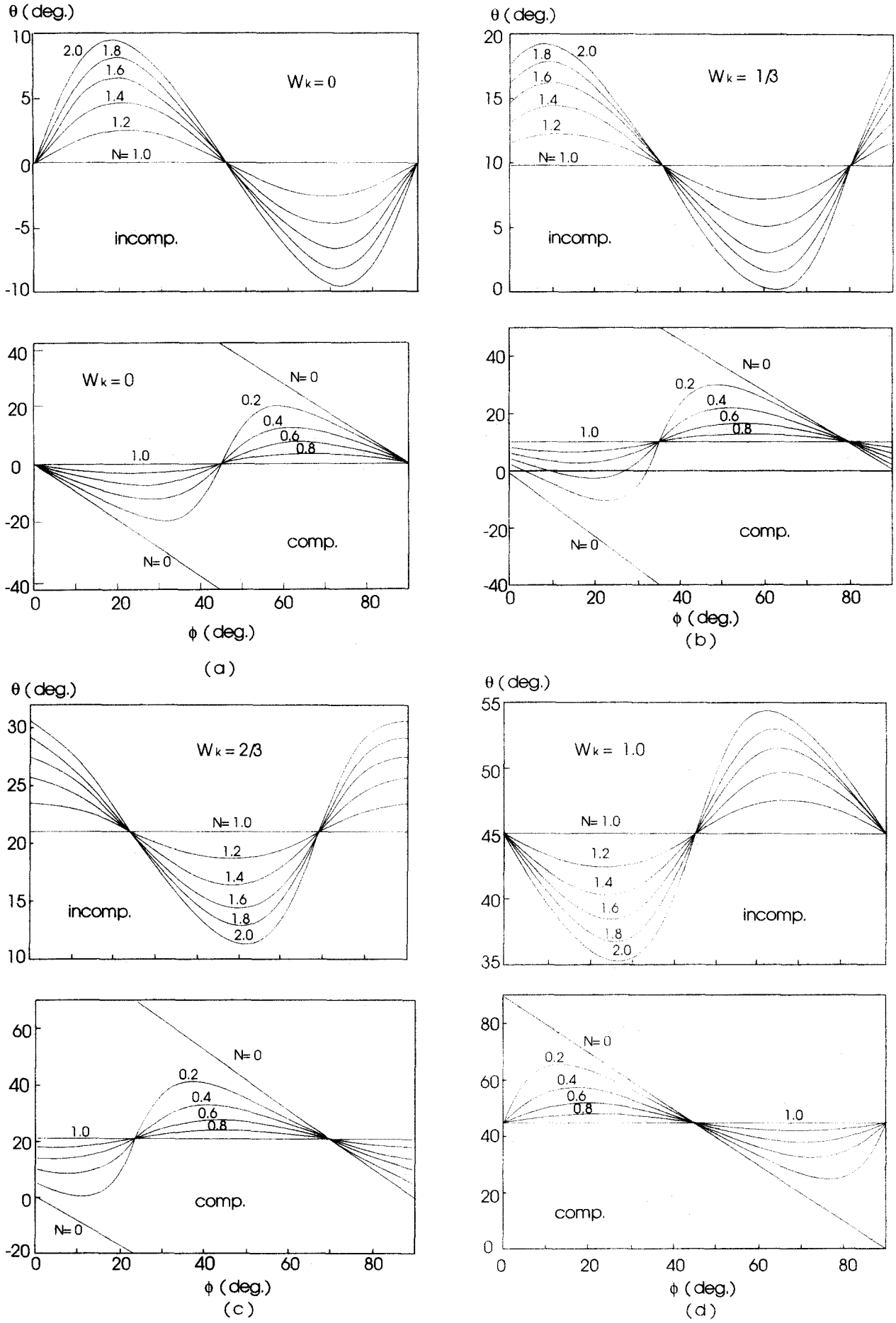

Fig. 5. The orientation θ of the ISA within a layer vs orientation ϕ of the layer with respect to the bulk flow field (upper: incompetent layers; lower: competent layers). For $\phi < 0$, we have $\theta(\phi) = \theta(90 + \phi)$. (a) $W_k = 0$, (b) $W_k = \frac{1}{3}$, (c) $W_k = \frac{2}{3}$ and (d) $W_k = 1$.

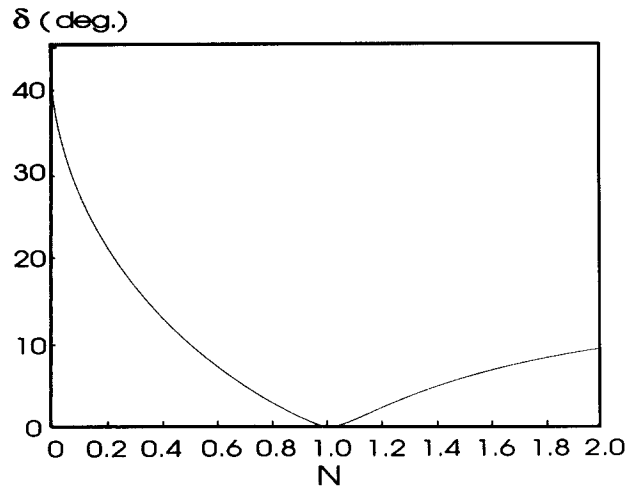

Fig. 6. The relationship between the maximum deviation (δ) of θ from ξ in different layers vs their competence factor. See text for details.

the more incompetent the layer (higher N), the more likely is reverse shear. For example for $W_k = 0$, all incompetent layers undergo reverse shear, but for $W_k = 2/3$, only layers with $N > 1.2$ undergo reverse shear, and for $W_k = 1$, only layers with $N > 1.4$ undergo reverse shear. For competent layers, the sense of shear is mostly sympathetic, but a strong reverse sense of shear occurs in the BR sector with the peak at B_2.

Variation of W_k'

The variation of W_k' is presented in Fig. 9. All flow regimes can occur in both incompetent and competent layers depending on the bulk kinematic vorticity number, competence factor and instantaneous orientation of the layer. When the bulk kinematic vorticity is relatively low (0 and 1/3), flow in incompetent layers is mostly sub-simple shear. As bulk kinematic vorticity increases (2/3 and 1) super-simple shear can occur in the whole incompetent layer. Flows in competent layers strongly tend to be super-simple shear. Peak W_k' is reached as the layer is near B_1 or B_2.

Comparison with Ishii's results

The results as presented in Figs. 5–9 generally agree with Ishii's figs. 3 and 5–7 (Ishii 1992) but are much more detailed. Most importantly, they clearly reveal the relationships between the 'eigen' directions of the bulk flow and the peaks of the curves. It is also evident that the introduction of a single quantity—the competence factor N—is advantageous over using two quantities—the viscosity ratio and thickness ratio.

DISCUSSION AND GEOLOGICAL IMPLICATIONS

Flow of rocks: heterogeneous and non-steady

Although rocks can, to some approximation (see Lister & Williams 1983, appendix I), be viewed as continua and hence the principles of continuum mechanics can often be applied, it should be borne in mind that rocks are far more heterogeneous and complex than any continua so far studied in continuum mechanics. In continuum mechanics theory, the decomposition of the velocity into three components (translation, pure deformation and vorticity) is often sufficient (Truesdell 1954, 1965, Sedov 1971). To describe flow of rocks however, the vorticity itself must be partitioned into two components and *non-coaxiality* is introduced as a concept different from *rotation*. The inescapable heterogeneity of rocks leads to uneven and time-dependent distribution of the velocity gradient tensor (Jiang 1994) and therefore to flow variations in space and time.

Figures 5–9 explicitly show flow variation in space (from layer to layer, varying N) and with time (as ϕ changes) even though the bulk flow is set constant (pure shear, sub-simple shear or simple shear).

Flow parameters in competent and incompetent layers have roughly inverse relationships. Reverse sense of non-coaxiality can occur in the same layer at different times or in different layers at the same time (Figs. 8 and 9). The suggestion by Lister & Williams (1983) that competent layers possibly have flowed more coaxially only holds for layers with $N = 0$. Generally, flow in competent layers can be highly non-coaxial at certain orientations (Fig. 9). The observation that in natural deformation competent domains usually have less finite strain than incompetent domains is either a result that flow in competent domains is less strong than in incompetent domains or that the finite strain in competent domains is accumulated less efficiently due to higher flow non-coaxiality or both.

Using flow parameters in Figs. 5 and 9, flow in a layer with $N = 2$ in a bulk flow field with $W_k = 2/3$ is constructed as an example to show how flow regime in a layer varies with time (Fig. 10). Flow in the layer can be sub-simple shear (a,b,c,h,m), simple shear (d,f,j,l), super-simple shear (e,k) and pure shear (g,i) depending on the instantaneous orientation of the layer. Therefore super-simple shear may be possible not only on grain scales (Means 1981, Talbot & Jackson 1987) or in the vicinities of deformable porphyroclasts (Simpson & De Paor 1993), but can also occur throughout a whole layer.

In addition to the competence factor of a layer N being time-dependent, the kinematic vorticity number for the bulk flow, W_k, may also be time-dependent due to bulk flow scale vorticity distribution and partitioning. Therefore the flow of a layer at any instant can be expressed as the following function:

$$\text{flow of a layer} = f(W_k, N, \phi). \quad (14)$$

Equation (14) explicitly shows the significant heterogeneity and non-steadiness of natural flows.

Structures related to the stretching histories of material lines

In a progressive deformation, ISA spinning and flow regime variation give rise to much more complicated

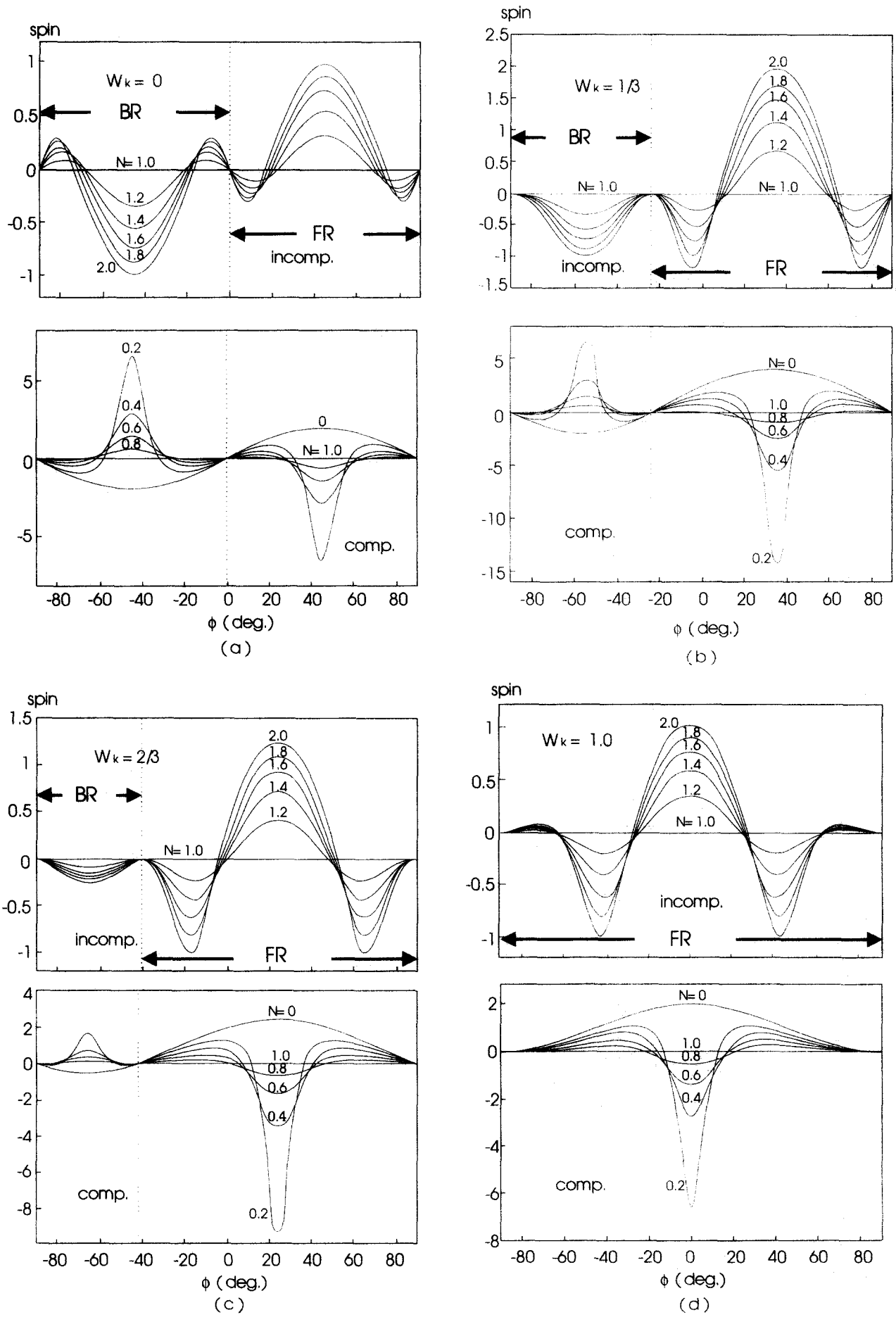

Fig. 7. Spin as a function of angle, ϕ, for various values of W_k and N. The main peaks in the curves show an approximate inverse relationship for incompetent and competent layers. See text for details.

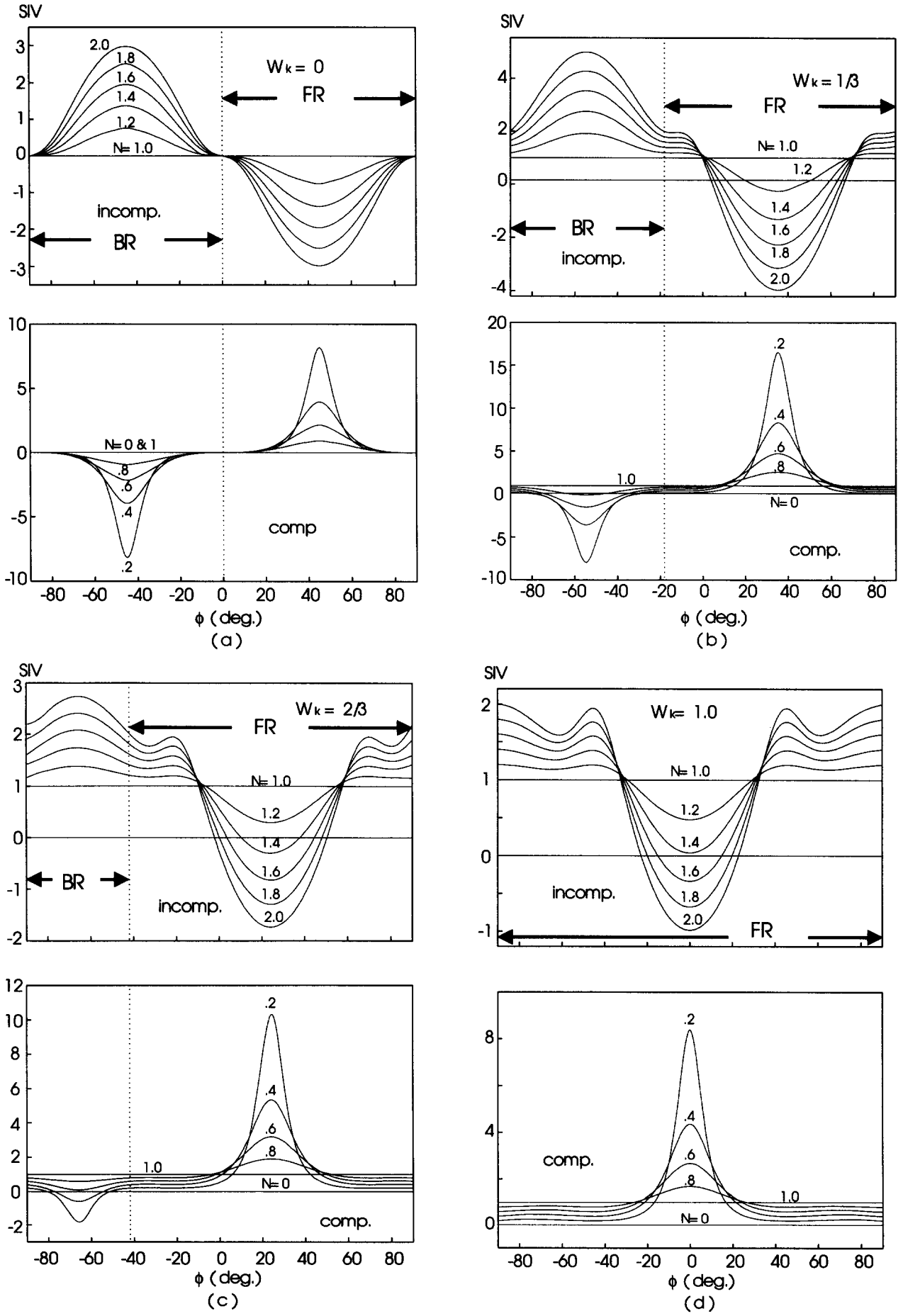

Fig. 8. SIV as a function of angle, ϕ, for various values of W_k and N. Again the main peaks in the curves show an approximate inverse relationship for incompetent and competent layers. A reverse sense of shear may occur in both incompetent and competent layers. See text for details.

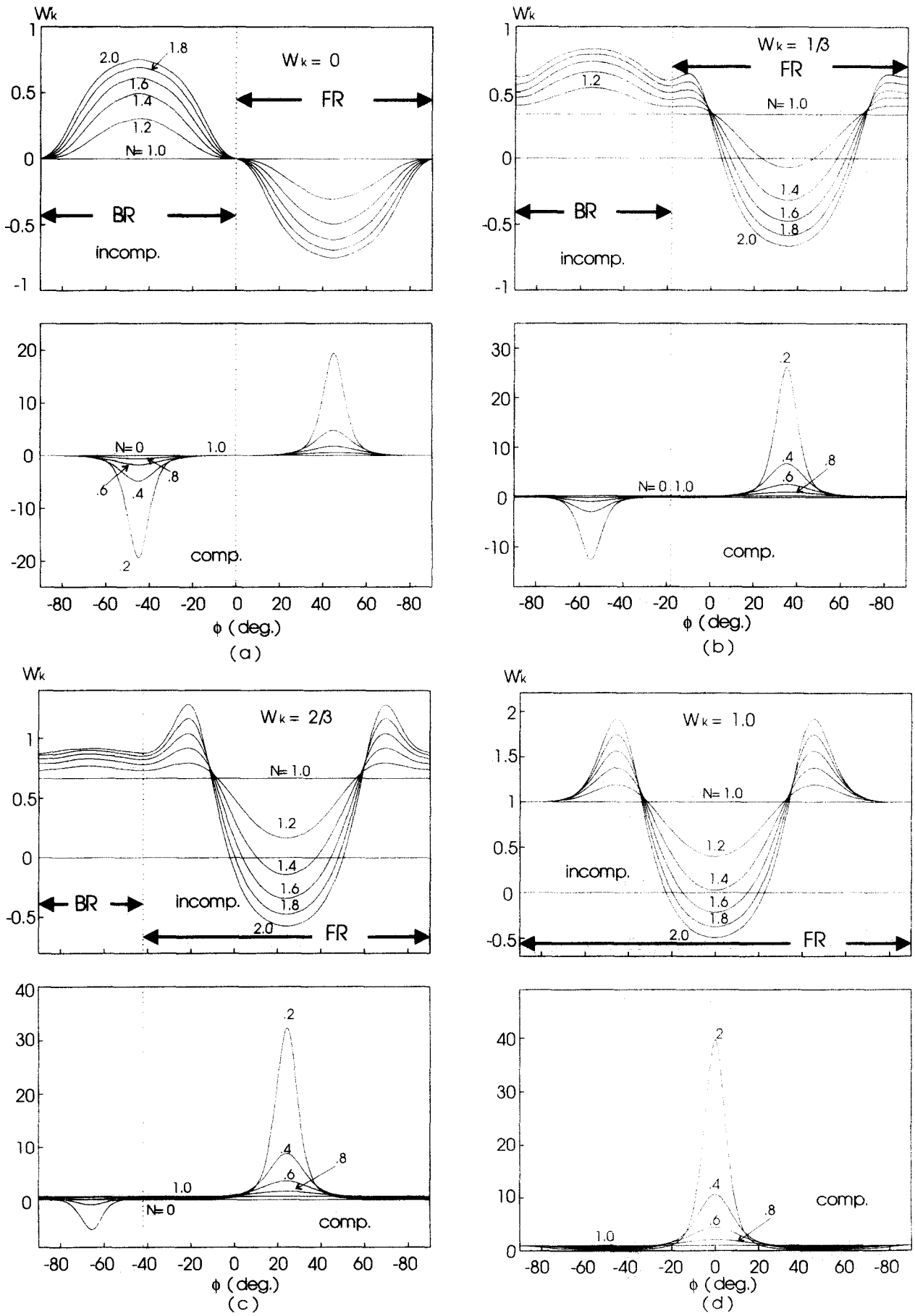

Fig. 9. W_k' as a function of angle, ϕ, for various values of W_k and N. Any flow regime can occur in both incompetent and competent layers. Reverse non-coaxiality can occur in the same layer at different times (varying ϕ) or in different layers (varying N) at the same time. Around B_1 and B_2, competent layers tend to be highly non-coaxial and super-simple shear. See text for details.

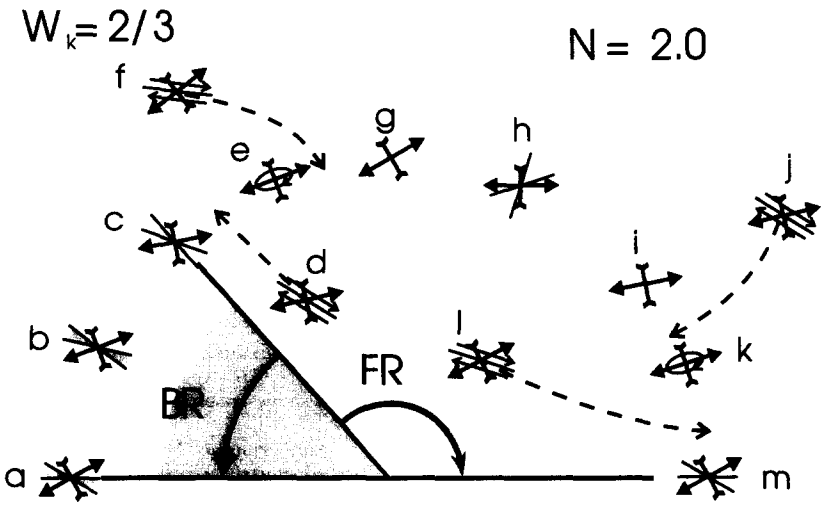

Fig. 10. Flow in a layer with $N = 2.0$ in a bulk flow field with $W_k = \frac{2}{3}$ constructed from data in Figs. 6 and 10. A variety of flow regimes can occur. See text for details.

stretching and rotation histories of material lines than those in non-spinning steady flow situations (Fig. 11). Because of ISA spinning, in a single deformation there exist not only material lines that, having undergone shortening in the past, will become extended in the future (se in Fig. 11a) (e.g. boudinaged folds), but also material lines that, having been extended in the past, will become shortened in the future (es in Fig. 11a) (e.g. folded boudins). The development of kink-band and shear-band cleavage in shear zones may not only be attributed to increasing strain and associated fabric build up and hardening (e.g. Platt & Vissers 1980, Gapais & White 1982) but may also result from the spinning of the ISA with respect to the foliation (see also Passchier 1991b). Shortened or folded boudins need not be a result of multi-deformational events or volume change (Von Brunn & Talbot 1986, Passchier 1990, Hanmer & Passchier 1991). Similarly the successive development of folds in shear zones (Platt 1983, Ghosh & Sengupta 1984, 1987, Hudleston 1989) can be easily interpreted as being due to the spinning of the ISA with respect to the fold plane.

Structures related to the rotation histories of material lines—a precautionary note on shear-sense indicators

As outlined earlier, material lines rotate differently in different flow regimes. The spinning of ISA and variation of flow regime lead to complex rotational histories of material lines: lines previously rotated forward may rotate backward (FB) and vice versa (BF) (Fig. 11b). Flow regime variation may change the relative rotation rate or even sense of rotation between porphyroclasts and foliation. For example, when a relatively rigid porphyroclast with an axial ratio more than a critical value undergoes flow variation from simple shear to subsimple shear, the rotation rate will certainly change, and if its long axis lies within the backward rotation sector, it will rotate backward. For certain N and ϕ, the reversal of the internal vorticity (Fig. 8) will reverse the sense of

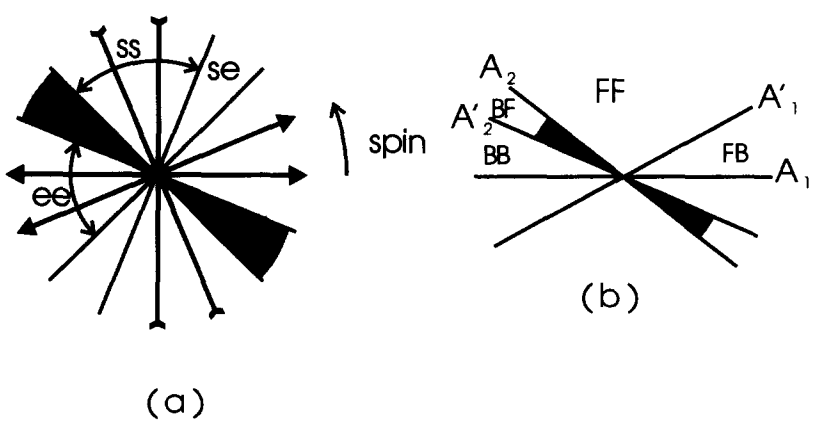

Fig. 11. Possible material line stretching (a) and rotation (b) histories as a result of ISA spinning and flow regime variation. (ee: Extended lines; se: shortened then extended lines; ss: shortened lines; es: extended then shortened lines; FF: forward rotation of lines; FB: forward then backward rotation of lines; BF: backward then forward rotation of lines; BB: backward rotation of lines.)

rotation of the porphyroclast. Any of these factors may contribute to the observed double rotation of porphyroclasts (Dixon 1976, Simpson & De Paor 1993).

Asymmetry of structures, especially porphyroclasts, have been used as shear-sense indicators (for a complete review see Hanmer & Passchier, 1991). As most structures, shear-sense indicators usually record a *local* and *incremental* strain history. They can only reflect the local kinematics of a period prior to the 'fossilization' of the structures. Since sense of shear varies in space and time in layered rocks and is expected to do so in rocks with any compositional and structural heterogeneities, development of inconsistent shear-sense indicators is not at all surprising in such rocks. To the contrary, consistence of shear-sense indicators in some areas may instead be anomalous special cases where relatively simple and homogeneous deformation has occurred (e.g. when $N = 1$), the assumption of which often creates unnecessary dilemmas and cannot in general be justified. The establishment of bulk kinematics relies on detailed structural analysis on different scales and is not always possible. For some complex metamorphic terrains, bulk kinematics may be as indeterminable as the stratigraphy. Directly relating a shear-sense indicator to bulk kinematics is dangerous.

Fabrics and flow 'eigen' directions

Fabrics in rocks represent incomplete memories of their past experience. They are developed through a variety of physicochemical processes. Structural geologists tend to consider fabrics in terms of strain and flow 'eigen' directions, e.g. to equate foliations to the XY planes of the finite strain (but see however, Williams 1972, 1977, Hobbs *et al.* 1982). Some fabric elements are thought to be instantaneous strain sensitive, such as quartz preferred orientation fabrics (Lister & Hobbs 1980), steady-state foliations (Means 1981), symmetry axes of rigid objects blocked in the flow (Ghosh & Ramberg 1976, Passchier 1987b). These fabric elements reflect the influence of the flow immediately prior to fossilization of the fabric (Lister & Hobbs 1980). As has been shown in this study, no flow 'eigen' directions including ISA are expected to be fixed in a progressive deformation. In incompetent layers with $N = 2$, spin can be twice the bulk shear strain rate and in competent layers, it can be more than 10 times (Fig. 7). It would be difficult for any fabric element materially defined to keep track of the elusive ISA. Even if some fabric elements do track the ISA, their orientations only indicate the fossilizing stages of the deformation. In layered rocks, there will be an uncertainty of $\pm 2\delta$ over which the ISA might have spinned.

Acknowledgements—I thank Drs P. F. Williams and J. C. White for critically reading an early draft of this paper, inspiring discussion and valuable suggestions. Review comments from Professor Peter Hudleston, P. R. Cobbold and an anonymous referee have been very helpful. Support from Natural Sciences and Engineering Research Council of Canada (NSERC) operating grant A8512 and a Lithoprobe Supporting Grant to J. C. White is acknowledged. This is Lithoprobe publication 493.

REFERENCES

Astarita, G. 1976. Objective and generally applicable criteria for flow classification. *J. Non-Newtonian Fluid Mech.* **6**, 69–76.
Bobyarchick, A. R. 1986. The eigenvalues of steady-state flow in Mohr space. *Tectonophysics* **122**, 35–51.
Celma, A. G. 1982. Domainal and fabric heterogeneities in the Cap de Creus quartz mylonites. *J. Struct. Geol.* **4**, 443–455.
Choukroune, P., Gapais, D. & Merle, O. 1987. Shear criteria and structural asymmetry. *J. Struct. Geol.* **9**, 525–530.
Cobbold, P. R. 1983. Kinematic and mechanical continuity at a coherent interface. *J. Struct. Geol.* **5**, 341–349.
De Paor, D. G. 1983. Orthographic analysis of geological structures—I. Deformation theory. *J. Struct. Geol.* **5**, 255–278.
Dixon, J. M. 1976. Apparent "double rotation" of porphyroblasts during a single progressive deformation. *Tectonophysics* **34**, 101–115.
Gapais, D. & White, S. H. 1982. Ductile shear bands in a naturally deformed quartzite. *Textures & Microstruct.* **5**, 1–17.
Ghosh, S. K. & Ramberg, H. 1976. Reorientation of inclusions by combination of pure shear and simple shear. *Tectonophysics* **34**, 1–70.
Ghosh, S. K. & Sengupta, S. 1984. Successive development of plane non-cylindrical folds in progressive deformation. *J. Struct. Geol.* **6**, 703–709.
Ghosh, S. K. & Sengupta, S. 1987. Progressive development of structures in a ductile shear zone. *J. Struct. Geol.* **9**, 277–289.
Goguel, J. 1979. Analyse théorique du chemin de la déformation, à gradient de vélocité permanent. *Tectonophysics* **60**, T17–T26.
Hanmer, S. & Passchier, C. W. 1991. Shear sense indicators: a review. *Geol. Surv. Can. Pap.* **90–117**.
Hobbs, B. E., Means, W. D. & Williams, P. F. 1976. *An Outline of Structural Geology*. John Wiley, New York.
Hobbs, B. E., Means, W. D. & Williams, P. F. 1982. The relationship between foliation and strain: an experimental investigation. *J. Struct. Geol.* **4**, 411–428.
Hudleston, P. J. 1989. The association of folds and veins in shear zones. *J. Struct. Geol.* **11**, 949–957.
Ishii, K. 1992. Partitioning of non-coaxiality in deforming rock masses. *Tectonophysics* **210**, 33–43.
Jiang, D. 1994. Vorticity determination, distribution, partitioning and the heterogeneity and non-steadiness of natural deformations. *J. Struct. Geol.* **16**, 121–130.
Kanagawa, K. 1993. Competence contrasts in ductile deformation as illustrated from naturally deformed chert-mudstone layers. *J. Struct. Geol.* **15**, 865–885.
Kirby, S. H. & Kronenberg, A. K. 1987. Rheology of the lithosphere: selected topics. *Rev. Geophys.* **25**, 1219–1244.
Lister, G. S. & Hobbs, B. E. 1980. The simulation of fabric development during plastic deformation and its application to quartzites. *J. Struct. Geol.* **2**, 355–370.
Lister, G. S. & Williams, P. F. 1979. Fabric development in shear zones: theoretical controls and observed phenomena. *J. Struct. Geol.* **1**, 283–297.
Lister, G. S. & Williams, P. F. 1983. The partitioning of deformation in flowing rock masses. *Tectonophysics* **92**, 1–33.
Means, W. D. 1981. The concept of steady-state foliation. *Tectonophysics* **78**, 179–199.
Means, W. D. 1990. Review paper—Kinematics, stress, deformation and material behavior. *J. Struct. Geol.* **12**, 953–972.
Means, W. D., Hobbs, B. E., Lister, G. S. & Williams, P. F. 1980. Vorticity and non-coaxiality in progressive deformations. *J. Struct. Geol.* **2**, 371–378.
Ottino, J. M. 1989. *The Kinematics of Mixing: Stretching, Chaos, and Transport*. Cambridge University Press, Cambridge.
Passchier, C. W. 1986. Flow in natural shear zones—the consequences of spinning flow regimes. *Earth Planet. Sci. Lett.* **77**, 70–80.
Passchier, C. W. 1987a. Efficient use of the velocity gradients tensor in flow modelling. *Tectonophysics* **136**, 159–163.
Passchier, C. W. 1987b. Stable positions of rigid objects in non-coaxial flow—a study in vorticity analysis. *J. Struct. Geol.* **9**, 679–690.
Passchier, C. W. 1988a. Analysis of deformation paths in shear zones. *Geol. Rdsch.* **77**, 309–318.
Passchier, C. W. 1988b. The use of Mohr circles to describe non-coaxial progressive deformation. *Tectonophysics* **149**, 323–338.
Passchier, C. W. 1990. Reconstruction of deformation and flow parameters from deformed vein sets. *Tectonophysics* **180**, 185–199.
Passchier, C. W. 1991a. The classification of dilatant flow types. *J. Struct. Geol.* **13**, 101–104.

Passchier, C. W. 1991b. Geometric constraints on the development of shear bands in rocks. *Geologie Mijnb.* **70**, 203–211.
Platt, J. P. 1983. Progressive refolding in ductile shear zones. *J. Struct. Geol.* **5**, 619–622.
Platt, J. P. & Vissers, R. L. M. 1980. Extensional structures in anisotropic rocks. *J. Struct. Geol.* **2**, 397–410.
Price, N. J. & Cosgrove, J. W. 1990. *Analysis of Geological Structures*. Cambridge University Press, Cambridge.
Ramberg, H. 1975. Particle paths, displacement and progressive strain applicable to rocks. *Tectonophysics* **28**, 1–37.
Ramsay, J. G. 1982. Rock ductility and its influence on the development of tectonic structures in mountain belts. In: *Mountain Building Processes* (edited by Hsu, K. J.). Academic Press, London, 111–127.
Ramsay, J. G. & Huber, M. I. 1983. *The Techniques of Modern Structural Geology, Volume*. 1: *Strain Analysis*. Academic Press, London.
Sedov, L. I. 1971. *A Course in Continuum Mechanics, Volume* I. *Basic Equations and Analytical Techniques*. Wolter-Noordhoff, Groningen.
Simpson, C. & De Paor, D. G. 1993. Strain and kinematic analysis in general shear zones. *J. Struct. Geol.* **15**, 1–20.
Talbot, C. J. & Jackson, M. A. 1987. Internal kinematics of salt diapirs. *Bull. Am. Ass. Petrol. Geol.* **71**, 1068–1098.
Tanner, R. I. 1976. A test particle approach to flow classification for viscoelastic fluids. *AIChE J.* **22**, 910–914.
Treagus, S. H. 1983. A theory of finite strain variation through contrasting layers, and its bearing on cleavage refraction. *J. Struct. Geol.* **5**, 351–368.
Treagus, S. H. 1988. Strain refraction in layered systems. *J. Struct. Geol.* **10**, 517–527.
Treagus, S. H. 1993. Flow variations in power-law multilayers: implications for competence contrasts in rocks. *J. Struct. Geol.* **15**, 423–434.
Treagus, S. H. & Sokoutis, D. 1992. Laboratory modelling of strain variation across rheological boundaries. *J. Struct. Geol.* **14**, 405–424.
Truesdell, C. A. 1954. *The Kinematics of Vorticity*. Indiana University Press, Bloomington.
Truesdell, C. A. 1965. *The Elements of Continuum Mechanics*. Springer, New York.
Tullis, T. E., Horowitz, F. G. & Tullis, J. 1991. Flow laws of polyphase aggregates from end-member flow laws. *J. geophys. Res.* **96**, 8081–8096.
Twiss, R. J. & Moores, E. M. 1992. *Structural Geology*. W. H. Freeman, New York.
Von Brunn, V, & Talbot, C. J. 1986. Formation of subglacial intrusive clastic sheets in the Dwyka formation of northern Natal, South Africa. *J. sedim. Petrol.* **56**, 35–44.
Weijermars, R. 1991. The role of stress in ductile deformation. *J. Struct. Geol.* **13**, 1061–1078.
Williams, P. F. 1972. Development of metamorphic layering and cleavage in low grade metamorphic rocks at Bermagui, Australia. *Am. J. Sci.* **272**, 1–47.
Williams, P. F. 1977. Foliation: a review and discussion. *Tectonophysics* **39**, 305–328.
Williams, P. F. & Schoneveld, C. 1981. Garnet rotation and the development of axial crenulation cleavage. *Tectonophysics* **78**, 307–334.

APPENDIX
DERIVATION OF L(t)

For some simple flows, the instantaneous velocity gradient tensor (**L**) is straightforward or can be easily determined. Integrating **L** gives the deformation gradient tensor **F** (Passchier 1988a,b, Weijermars 1991). For some complex flow situations, like those studied in this paper, the deformation gradient tensor may be relatively easier to derive. A reverse procedure is thus used: first derive **F** and then derive **L** from **F** by using the relations given by Truesdell (1965):

$$\mathbf{L}(t) = \dot{\mathbf{F}}(t) \cdot \mathbf{F}^{-1}(t) \tag{A1}$$

or

$$\mathbf{L}(t) = \lim_{\tau \to t} \dot{\mathbf{F}}_\tau(t), \tag{A2}$$

where $\mathbf{F}_\tau(t)$ means the incremental deformation gradient from time τ to time t.

For convenience of mathematical derivation, an external frame is established with x_1 parallel to A_1. In such a frame, $\mathbf{L}(t)$ is the sum of two components: $\mathbf{L}_\varepsilon$—a component contributed by the pure shear component of the bulk flow, and $\mathbf{L}_\gamma$—a component contributed by the simple shear component of the bulk flow.

Figure A1 shows a layer with competence factor N originally at an arbitrary angle ϕ_0 with respect to x_2 (ϕ_0-configuration, Fig. A1a) incrementally deformed into the ϕ-configuration (Fig. A1b). ψ_0 and ψ are defined so that $\tan(\psi_0) = N\tan(\phi_0)$ and $\tan(\psi) = N\tan(\phi)$. Figures A1(c) & (d) are Mohr circles of bulk shear flow and bulk simple shear flow, respectively, from which resolved shear strain rate parallel to the layer, layer-parallel stretching and angular velocity of the layer can be

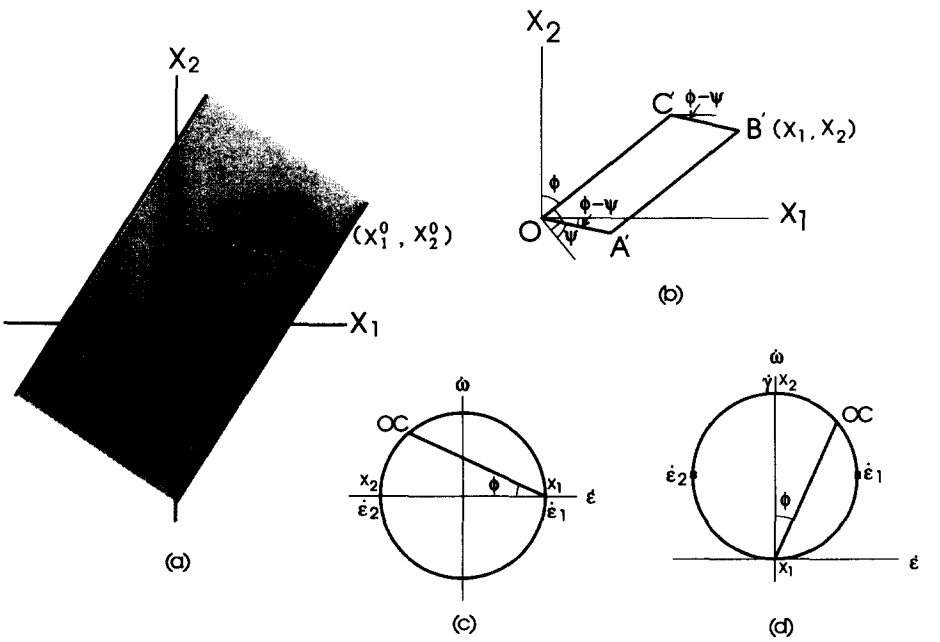

Fig. A1. (a) A layer with competence factor N in a pure shear or simple shear flow field. (b) After an incremental deformation, OABC becomes OA′B′C′. (c) & (d) Mohr circles of pure shear and simple shear, respectively, from which the layer-parallel (OC) stretching rate and resolved shear strain rate parallel to the layer can be obtained.

easily obtained (see Bobyarchik 1986, Passchier 1988, 1991a, Simpson & De Paor 1993).

Derivation of $\mathbf{L}_\varepsilon$

An arbitrary point B with co-ordinates (x_1^0, x_2^0) can thus be expressed as:

$$x_1^0 = \mathrm{OC}\sin\phi_0 + \mathrm{OA}\cos(\phi_0 - \psi_0)$$
$$x_2^0 = \mathrm{OC}\cos\phi_0 - \mathrm{OA}\sin(\phi_0 - \psi_0)$$

or in matrix form:

$$\begin{bmatrix} x_1^0 \\ x_2^0 \end{bmatrix} = \begin{bmatrix} \sin\phi_0 & \cos(\phi_0 - \psi_0) \\ \cos\phi_0 & -\sin(\phi_0 - \psi_0) \end{bmatrix} \begin{bmatrix} \mathrm{OC} \\ \mathrm{OA} \end{bmatrix}. \tag{A3}$$

After an incremental deformation, B become $\mathrm{B}'(x_1, x_2)$. Similarly, we have:

$$\begin{bmatrix} x_1 \\ x_2 \end{bmatrix} = \begin{bmatrix} \sin\phi & \cos(\phi - \psi) \\ \cos\phi & -\sin(\phi - \psi) \end{bmatrix} \begin{bmatrix} \mathrm{OC}' \\ \mathrm{OA}' \end{bmatrix}. \tag{A4}$$

Suppose $\lambda_\phi^{1/2}$ is the incremental stretch of the material line OC, i.e.:

$$\mathrm{OC}' = \lambda_\phi^{1/2}\,\mathrm{OC}. \tag{A5}$$

Obviously, we have:

$$\lim_{\phi_0 \to \phi} \lambda_\phi^{1/2} = 1.$$

For isochoric deformation, we have:

$$\mathrm{OA}' = \mathrm{OA}\lambda_\phi^{-1/2}\cos\psi_0/\cos\psi. \tag{A6}$$

Incorporating (A3), (A5), (A6) into (A4) and rearranging, we obtain the incremental deformation tensor from ϕ_0 configuration to ϕ configuration:

$$\mathbf{F}^\varepsilon_{\phi_0}(\phi) = \begin{bmatrix} \lambda_\phi^{1/2}\sin\phi & \lambda_\phi^{-1/2}\cos\psi_0\,(\cos\phi + N\sin\phi\tan\phi) \\ \lambda_\phi^{1/2}\cos\phi & -\lambda_\phi^{1/2}\cos\psi_0\sin\phi\,(1 - N) \end{bmatrix}$$
$$\begin{bmatrix} \dfrac{\sin(\phi_0 - \psi_0)}{\cos\psi_0} & \dfrac{\cos(\phi_0 - \psi_0)}{\cos\psi_0} \\ \dfrac{\cos\phi_0}{\cos\psi_0} & -\dfrac{\sin\phi_0}{\cos\psi_0} \end{bmatrix}. \tag{A7}$$

According to equation (A2), the instantaneous velocity gradient tensor in bulk pure shear, expressed in terms of ϕ, $\mathbf{L}_\varepsilon(\phi)$ is:

$$\mathbf{L}_\varepsilon(\phi) = \lim_{\phi_0 \to \phi} \dot{\mathbf{F}}^\varepsilon_{\phi_0}(\phi). \tag{A8}$$

From Fig. A1(c), it is readily seen that:

$$\lim_{\phi_0 \to \phi} \frac{\mathrm{d}\lambda_\phi^{1/2}}{\mathrm{d}t} = \dot{\varepsilon}(\phi) = -\dot{\varepsilon}\cos 2\phi, \qquad \frac{\mathrm{d}\phi}{\mathrm{d}t} = \dot{\varepsilon}\sin 2\phi.$$

$\mathbf{L}_\varepsilon(\phi)$ can be obtained.

Derivation of $\mathbf{L}_\gamma$

In the case of bulk simple shear, if the $\phi = 0$ configuration is chosen as the reference, we have:

$$x_1 = x_1^0\frac{\cos\phi}{\cos\psi}\cos(\phi - \psi) + \tan\phi\, x_2^0$$

$$x_2 = x_2^0 - x_1^0\frac{\cos\phi}{\cos\psi}\sin(\phi - \psi)$$

or in matrix form:

$$\begin{bmatrix} x_1 \\ x_2 \end{bmatrix} = \begin{bmatrix} \dfrac{\cos\phi}{\cos\psi}\cos(\phi - \psi) & \tan\phi \\ -\dfrac{\cos\phi}{\cos\psi}\sin(\phi - \psi) & 1 \end{bmatrix} \begin{bmatrix} x_1^0 \\ x_2^0 \end{bmatrix}.$$

After simplification, the deformation gradient tensor from the ϕ_0-configuration to the ϕ-configuration is:

$$\mathbf{F}_0(\phi) = \begin{bmatrix} N + (1 - N)\cos^2\phi & \tan\phi \\ -0.5\,(1 - N)\sin 2\phi & 1 \end{bmatrix}. \tag{A9}$$

If the ϕ_0-configuration is chosen as the reference, the transformation matrix from the ϕ_0-configuration to the ϕ-configuration is (see Jiang in press) $\mathbf{F}_0^{-1}(\phi_0)$. Therefore the deformation gradient tensor for the incremental deformation from the ϕ_0-configuration to the ϕ-configuration is:

$$\mathbf{F}^\gamma_{\phi_0}(\phi) = \mathbf{F}_0(\phi)\mathbf{F}_0^{-1}(\phi_0). \tag{A10}$$

Differentiating (A10) and incorporating $\mathrm{d}\phi/\mathrm{d}t = \dot{\gamma}\cos^2\phi$ (from Fig. A1d), the instantaneous velocity gradient tensor in bulk simple shear expressed in terms of ϕ can be obtained from:

$$\mathbf{L}_\gamma(\phi) = \lim_{\phi_0 \to \phi} \dot{\mathbf{F}}^\gamma_{\phi_0}(\phi). \tag{A11}$$

Therefore the instantaneous velocity gradient tensor $\mathbf{L}(t)$, being the sum of the pure shear and simple shear components is:

$$\mathbf{L}(\phi) = \mathbf{L}_\varepsilon(\phi) + \mathbf{L}_\gamma(\phi). \tag{A12}$$